

Orientation of ground-state orbital in CeCoIn₅ and CeRhIn₅

M. Sundermann,^{1,2} A. Amorese,^{1,2} F. Strigari,^{1,*} M. W. Haverkort,³ L. H. Tjeng,²
M. Moretti Sala,^{4,†} H. Yavaş,^{5,‡} E. D. Bauer,⁶ P. F. S. Rosa,⁶ J. D. Thompson,⁶ and A. Severing^{1,2}

¹*Institute of Physics II, University of Cologne, Zùlpicher StraÙe 77, 50937 Cologne, Germany*

²*Max Planck Institute for Chemical Physics of Solids, Nöthnitzer StraÙe 40, 01187 Dresden, Germany*

³*Institute for Theoretical Physics, Heidelberg University, Philosophenweg 19, 69120 Heidelberg, Germany*

⁴*European Synchrotron Radiation Facility, 71 Avenue des Martyrs, CS40220, F-38043 Grenoble Cedex 9, France*

⁵*PETRA III, Deutsches Elektronen-Synchrotron (DESY), NotkestraÙe 85, 22607 Hamburg, Germany*

⁶*Los Alamos National Laboratory, New Mexico 87545, USA*

(Dated: January 27, 2023)

We present core level non-resonant inelastic x-ray scattering (NIXS) data of the heavy fermion compounds CeCoIn₅ and CeRhIn₅ measured at the Ce $N_{4,5}$ -edges. The higher than dipole transitions in NIXS allow determining the orientation of the Γ_7 crystal-field ground-state orbital within the unit cell. The crystal-field parameters of the CeMIn₅ compounds and related substitution phase diagrams have been investigated in great detail in the past; however, whether the ground-state wavefunction is the Γ_7^+ ($x^2 - y^2$) or Γ_7^- (xy orientation) remained undetermined. We show that the Γ_7^- doublet with lobes along the (110) direction forms the ground state in CeCoIn₅ and CeRhIn₅. A comparison is made to the results of existing DFT+DMFT calculations.

I. INTRODUCTION

At high temperature, heavy-fermion materials are described by decoupled localized f electrons and conduction electron bands. Upon cooling, the localized f electrons start to interact with the conduction electrons (cf -hybridization) and become partially delocalized. The resulting entangled fluid consists of heavy quasiparticles with masses up to three orders of magnitude larger than the free electron mass. These quasiparticles may undergo magnetic or superconducting transitions. In the Doniach phase diagram temperature T versus exchange interaction \mathcal{J} , magnetic order prevails for small \mathcal{J} whereas a non-magnetic Kondo singlet state forms for large \mathcal{J} . Between these two regimes quantum critical behaviour occurs which is often accompanied by a superconducting dome that hides a quantum critical point (QCP).^{1,2} Understanding how these quasiparticles, that have atomic-like as well as itinerant character, give rise to these ground states is a challenging question in condensed-matter physics, and the answer to this question will provide predictive understanding of these quantum states of matter.³

The tetragonal compounds CeMIn₅ ($M = \text{Co}, \text{Rh}, \text{Ir}$) are heavy fermion compounds that display different ground states for different transition metal ions; for $M = \text{Co}$ and Ir the ground state is superconducting ($T_c = 2.3$ and 0.4 K) and for $M = \text{Rh}$ it is antiferromagnetic ($T_N = 3.8$ K).⁴ High-quality CeMIn₅ crystals can be grown, making this family suitable for determining the parameter that drives the different ground states. Within the above mentioned extended Doniach phase diagram, CeRhIn₅ is on the weak side of hybridization, CeCoIn₅ close to the QCP and CeIrIn₅ is on the side of stronger cf -hybridization, i.e. superconductivity goes along with stronger cf -hybridization. Although there are strong indications for localization (Rh) and delocalization (Co, Ir) in, e.g., the size of the Fermi surface,^{5–12} it is not possible

to detect the differences in f occupations. They are so subtle that they are below the detection limit.¹³

A light-polarization analysis of soft X-ray absorption spectra shows that the crystal-field wavefunction of the ground state correlates with the ground state properties in the temperature-transition metal (substitution) phase diagram of CeCoIn₅-CeRhIn₅-CeRh_{1- δ} Ir _{δ} In₅-CeIrIn₅; orbitals more compressed in the tetragonal ab -plane favour an antiferromagnetic ground state as for CeRhIn₅ and the Rh rich compounds with $\delta \leq 0.2$. The compounds with more elongated orbitals along the c axis, however, have superconducting ground states (CeCoIn₅, CeIrIn₅ and also the Ir rich compounds with $\delta \geq 0.7$).^{14,15} The obvious conclusion is that the more pronounced extension of the ground state orbitals in the direction of quantization (crystallographic c direction) promotes stronger hybridization in c direction since superconductivity goes along with stronger hybridization. This is supported by combined local density approximation plus dynamical mean field theory (LDA+DMFT) calculations by Shim *et al.*¹⁶ that find for CeIrIn₅ the strongest hybridization with the out-of-plane In(2) ions (see unit cell in Fig. 1 (a)). It was also shown that the suppression of superconductivity in CeCo(In_{1- y} Sn _{y})₅ by about 3% of Sn is due to a homogeneous increase of hybridization in the tetragonal ab plane since the Sn ions go preferably to the In(1) sites.¹⁷ Accordingly, we found that here the hybridization with In(1) ions plays a decisive role; the $4f$ ground state orbital extends increasingly in the plane as the Sn content is increased.¹⁸

Hence, the ground state wavefunction is a very sensitive probe for quantifying hybridization. Haule *et al.* obtained a $4f$ Weiss field hybridization function for CeMIn₅ based on realistic lattice parameters using density functional theory plus dynamical mean field (DFT+DMFT) calculations which they have decomposed into crystal-field components.¹⁹ Here our goal is to verify that the crystal-field components that were extracted in these cal-

culations are in agreement with reality.

The tetragonal point symmetry of Ce in CeMIn_5 splits the Ce Hund's rule ground state into three Kramers doublets, two Γ_7 doublets $\Gamma_7^{+/-} = |\alpha| |\pm 5/2\rangle + / - \sqrt{1 - \alpha^2} |\mp 3/2\rangle$ and $\Gamma_7^{-/+} = \sqrt{1 - \alpha^2} |\pm 5/2\rangle - / + |\alpha| |\mp 3/2\rangle$, and one $\Gamma_6 = |\mp 1/2\rangle$. We write $+/-$ or $-/+$ because the sign has not yet been determined, and this is the scope of the present manuscript. Γ_6 as a pure J_z state has full rotational symmetry around the quantization axis c but the mixed states have lobes with fourfold rotational symmetry. The magnitude of α describes the extension of the $\Gamma_7^{+/-}$ orbitals in c direction whereby the sign in the wavefunction determines how the orbitals are oriented within the unit cell; with the lobes along $[100]$ (Γ_7^+ : $x^2 - y^2$) or with the lobes along $[110]$ (Γ_7^- : xy). Figure 1 (b) shows the scenario of a Γ_7^- ground state and Γ_7^+ excited state for several α^2 values. Figure 1 (c) shows the same for a Γ_7^+ ground and excited Γ_7^- -state.

The crystal-field potential of the CeMIn_5 has been determined with inelastic neutron scattering (INS)^{20,21} and the ground state wavefunctions were studied in greater detail with linear polarized soft x-ray absorption spectroscopy.^{15,18,22} Hence, the crystal-field energy splittings, the sequence of states ($\Gamma_7^{+/-}$, $\Gamma_7^{-/+}$, Γ_6) and also the magnitude of the α -values are known (0.36, 0.62, 0.5 for Co, Rh and Ir). Only the sign of the wavefunction remains unknown because it cannot be determined with any of these dipole-selection-rule based spectroscopies. We, therefore, set up an experiment to determine the sign of the ground-state wave function in the CeMIn_5 compounds in order to find out which one of the two scenarios in Fig. 1 (a) applies.

II. METHOD

We performed a core level non-resonant inelastic x-ray scattering (NIXS) experiment at the Ce $N_{4,5}$ -edges ($4d \rightarrow 4f$). It has been shown previously that this method is able to detect anisotropies with higher than twofold rotational symmetry.²³⁻²⁸ In the following, we briefly recap the principles of NIXS, a photon-in photon-out technique with hard x-rays ($E_{\text{in}} \approx 10$ keV). Because of the high incident energies, NIXS is bulk sensitive and allows one to reach large momentum transfers $|\vec{q}|$ of the order of 10 \AA^{-1} when measuring in back scattering geometry. At such large momentum transfers, the transition operator in the scattering function $S(\vec{q}, \omega)$ can no longer be truncated after the dipole term. As a result, higher order scattering terms contribute to the scattering intensity.^{23,29-33} For a $d \rightarrow f$ transition at about 10 \AA^{-1} , octupole (rank $k=3$) and triakontadipole ($k=5$) terms dominate the scattering intensity whereas the dipole part ($k=1$) is less prominent. Accordingly, the directional dependence of the scattering function in a single crystal experiments follows multipole selection rules, in analogy to the dipole selection rules in a linearly polarized x-ray

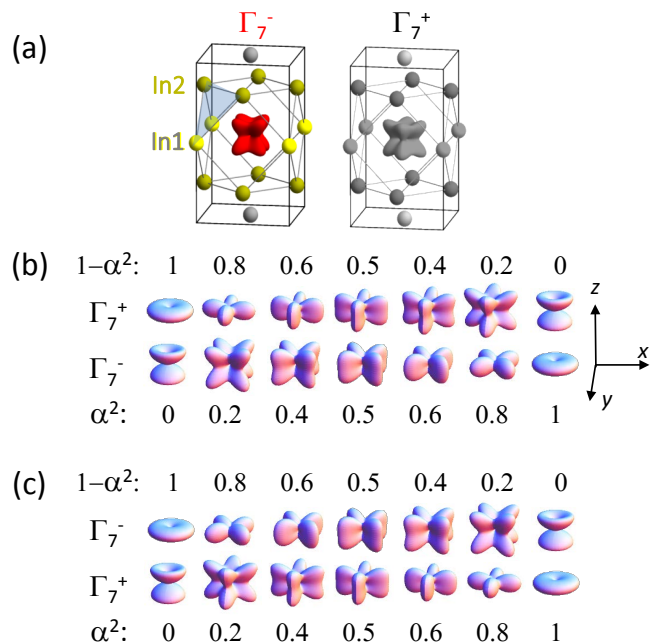


FIG. 1. (color online) top panel a) Unit cell of CeMIn_5 , for a Γ_7^- and a Γ_7^+ Ce ground state orbital. The light blue triangle emphasizes the In2-In1-In2 triangle. Middle panel b) $\Gamma_7^- = |\alpha| |\pm 5/2\rangle - \sqrt{1 - \alpha^2} |\mp 3/2\rangle$ ground state and $\Gamma_7^+ = \sqrt{1 - \alpha^2} |\pm 5/2\rangle + |\alpha| |\mp 3/2\rangle$ excited state; bottom panel c) $\Gamma_7^+ = |\alpha| |\pm 5/2\rangle + \sqrt{1 - \alpha^2} |\mp 3/2\rangle$ ground state with corresponding $\Gamma_7^- = \sqrt{1 - \alpha^2} |\pm 5/2\rangle - |\alpha| |\mp 3/2\rangle$ excited state for several values of α^2 , respectively.

absorption experiment. Thus single crystal NIXS yields information not only about the orbital occupation but also the sign of the wavefunction that distinguishes the xy and $x^2 - y^2$ orientations of a Γ_7 .

III. EXPERIMENT

CeCoIn_5 and CeRhIn_5 single crystals were grown using the standard In-flux technique. CeCoIn_5 crystals are plate-like with the $[001]$ direction perpendicular to the plate, whereas CeRhIn_5 crystals are more three-dimensional. All samples were aligned by Laue diffraction before the experiment. For each compound two samples were cut, one with a (100) and a second one with a (110) surface so that specular geometry could be realized in the experiment.

The experiments were performed at the NIXS end stations of two beamlines, ID20³⁴ at the European Synchrotron Radiation Facility (ESRF) in Grenoble, France and the Max-Planck P01 at PETRA III/DESY in Hamburg, Germany. CeCoIn_5 was measured at ID20. The ID20 set up was as follows: the incident energy is scanned using a double Si(111) monochromator and the energy of the scattered intensity was set to $E_{\text{final}} = 9690$ eV. The scattered intensity was analyzed by three columns of three Si(660) analyzers (in total nine)

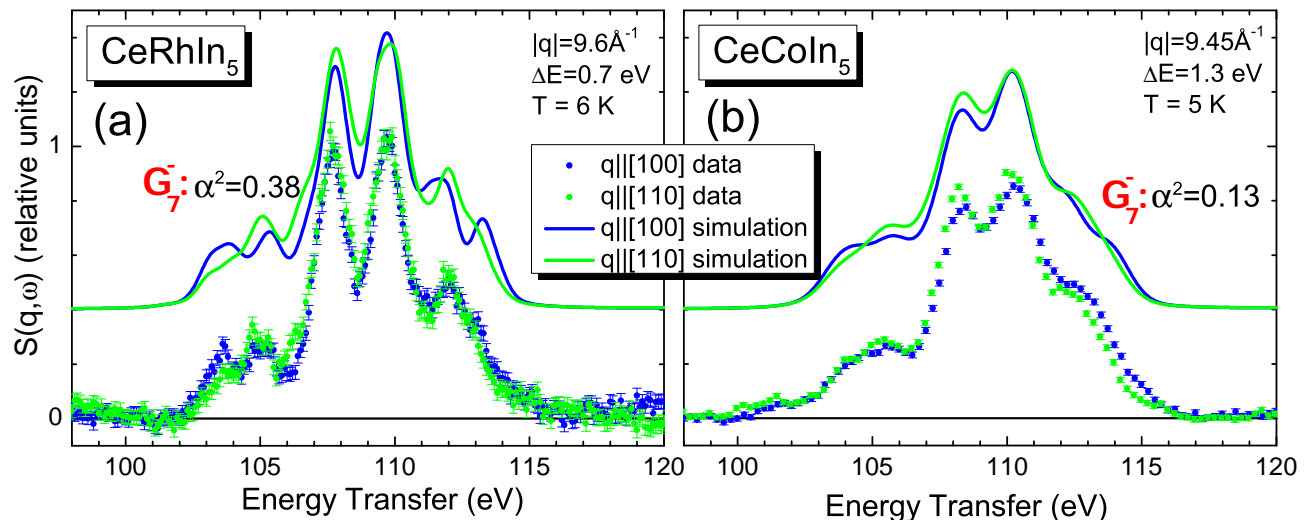


FIG. 2. (color online) Non resonant inelastic x-ray scattering (NIXS) spectra of CeCoIn₅ (left) and CeRhIn₅ (right) at the Ce $N_{4,5}$ -edges for the two crystallographic directions $\vec{q} \parallel [100]$ blue and $\vec{q} \parallel [110]$ green at low temperatures with different resolutions; dots data and lines simulations for a Γ_7^- state (xy orientation) (see text).

at *in-plane* scattering angles of $2\Theta = 140^\circ, 146^\circ,$ and 153° , corresponding to an averaged momentum transfer of $|\vec{q}| = 9.4 \pm 0.15 \text{ \AA}^{-1}$. CeRhIn₅ was measured at P01 with a slightly different set up; the resolution was better and the scattering geometry was vertical so that the polarization vector of the incoming light was vertical to the scattering plane. At P01 the incident energy was selected with a Si(311) double monochromator and twelve Si(660) 1 m radius spherically bent crystal analyzers were arranged in 3×4 array as shown in Fig. 2 of Ref. 26 so that the fixed final energy was the same as at ID20. The analyzers were positioned at scattering angles of $2\theta \approx 150^\circ, 155^\circ,$ and 160° which provide an averaged momentum transfer of $|\vec{q}| = 9.6 \pm 0.1 \text{ \AA}^{-1}$. At both beamlines the scattered beam was detected by a position sensitive custom-made detector (MAXIPIX at ID20, LAMBDA at P01), based on a Medipix3 chip detector. The elastic line was consistently measured and a pixel-wise calibration yields instrumental energy resolutions of $\approx 1.3 \text{ eV}$ at ID20 and $\approx 0.7 \text{ eV}$ full width at half maximum (FWHM) at P01. The improved resolution costs about a factor of five in intensity. Two samples of CeCoIn₅ and CeRhIn₅ were measured, one with a (100) and one with a (110) surface so that specular geometry for $\vec{q} \parallel [001]$ and $\vec{q} \parallel [110]$ could be realized.

We used the full multiplet code *Quanty*³⁵ for simulating the NIXS data. A Gaussian broadening of 1.3 eV accounts for the instrumental resolution of the ID20 data (CeCoIn₅) and of 0.7 eV for the P01 spectra (CeRhIn₅). An additional Lorentzian broadening of 0.4 eV FWHM accounts for life-time effects. The atomic parameters were taken from the Cowan code,³⁶ whereby the Hartree-Fock values of the Slater integrals were reduced to about 60% for the $4f-4f$ and to about 80% for the $4d-4f$ Coulomb interactions to reproduce the energy distribu-

tion of the multiplet excitations of the Ce $N_{4,5}$ -edges. This reduction accounts for configuration interaction processes not included in the Hartree-Fock scheme.³⁷

IV. RESULTS

Figure 2 shows NIXS data (dots) at the Ce $N_{4,5}$ -edges of CeRhIn₅ (a) and CeCoIn₅ (b) plus simulations (lines) for two scattering directions, $\vec{q} \parallel [100]$ (blue) and $\vec{q} \parallel [110]$ (green). The CeRhIn₅ data have more structure than the CeCoIn₅ data since they were taken with better resolution, but the overall shape of the spectra looks very similar and represents the multipole scattering expected for the Ce $N_{4,5}$ -edges.^{23–26,30}

We discuss first the simulations in order to show what directional effect to expect due to the in-plane anisotropy of the Γ_7 orbital. The simulations in Fig. 2 have been performed for ground states with Γ_7^- (xy) orientation,

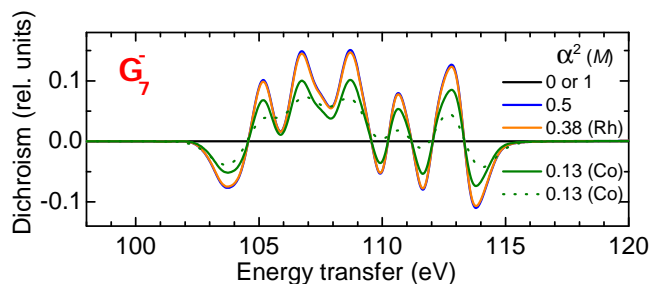


FIG. 3. (color online) Simulated difference spectra $I_{\vec{q} \parallel [110]} - I_{\vec{q} \parallel [100]}$ (dichroism) for α^2 values of 0 (1) and 0.5, and of 0.38 for CeRhIn₅ and 0.13 for CeCoIn₅; the solid lines account for an energy resolution of 0.7 eV, the dotted line of 1.3 eV.

taking into account the respective J_z admixtures (α^2 values) and resolutions. The directional dependence shows clearly below 105 eV where the scattering for $\vec{q} \parallel [100]$ (blue) is stronger than for $\vec{q} \parallel [110]$ (green), i.e. the simulations show blue over green. At 105 eV the two intensities cross and at further increasing energy transfers green is stronger than blue. Especially at about 108 eV the scattering for $\vec{q} \parallel [110]$ (green) is stronger, and at the falling tale of the edge at about 112 eV both intensities cross again.

In Figure 3, we compare the directional dependence $I_{\vec{q} \parallel [110]} - I_{\vec{q} \parallel [100]}$ (dichroism) for several α^2 values. For $\alpha^2 = 0$ or 1 the dichroism is zero because in this case the Γ_7 state is a pure J_z state and rotational invariant; for $\alpha^2 = 0.5$ the dichroism is largest. For CeRhIn₅ ($\alpha^2 = 0.38$) the mixing factor α^2 is closer to 0.5 than for CeCoIn₅ ($\alpha^2 = 0.13$) so that the expected dichroism is larger in the former. For a Γ_7^+ ground state the intensities are simply opposite so that the present experiment yields an either positive or negative result; a positive (negative) dichroism at a certain energy transfers yields the sign of the wavefunction, i.e. the interpretation of the data is straight forward.

We now start comparing data and simulation of CeRhIn₅ in Fig. 2 (a). The dichroism of the pre-edge, the crossing of intensities at 105 eV, the stronger scattering for $\vec{q} \parallel [110]$ at 108 eV, and also the dichroism and crossing of intensities at about 112 eV are very well reproduced with the Γ_7^- simulation.

For CeCoIn₅ the effect is weaker as expected. According to the simulations in Fig. 3 the dichroism should amount to only about 60% of the dichroism of CeRhIn₅ (compare red and green solid lines). In addition, in the CeCoIn₅ experiment the resolution was worse so that the dichroism is more washed out (compare dotted green line in Fig. 3) and the magnitude $|\vec{q}|$ of the momentum transfer is slightly smaller than in the set-up at P01 for CeRhIn₅. Nevertheless, the crossing of intensities and the stronger scattering for $\vec{q} \parallel [110]$ at 108 eV strongly suggests that also here the Γ_7^- is the ground state. Especially here, the fact that we are dealing with an either-or experiment helps the interpretation.

V. DISCUSSION

Figure 4 summarizes what we know about the crystal-field splittings of the $J = 5/2$ multiplet of CeMIn₅. The splittings and α^2 values are taken from inelastic neutron scattering and x-ray absorption as published in Ref. 20–22. NIXS experiments on CeCoIn₅ and CeRhIn₅ add the information that the Γ_7^- is the ground state for both compounds, i.e. the lobes of the ground state are along the crystallographic (110) direction. These Γ_7^- ground state orbitals extend more in z -direction than the Γ_7^+ at about 6-7 meV. The Γ_7^+ , especially for CeCoIn₅, extend mostly in the xy plane so that they do not point to the out-of-plane In2 ions as suggested by Haule *et al.*¹⁹

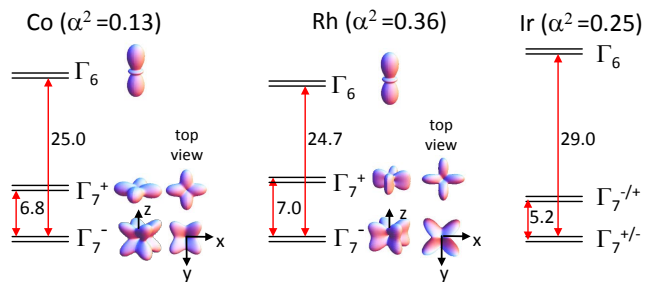


FIG. 4. (color online) Crystal-field splitting of $J = 5/2$ multiplet of CeCoIn₅, CeRhIn₅ and for completeness of CeIrIn₅ as adapted from Ref.s 20–22. For $M = \text{Co}$ and Rh the sign of the wavefunction is now determined which has been taken into account when drawing the f^2 charge densities of the respective states.

The tips of the lobes of the Γ_7^- ground state wavefunctions of CeCoIn₅ and CeRhIn₅ are pointing towards the triangle In2-In1-In2 (coloured unit cell in Fig. 1). It is therefore reasonable to conclude that the impact of the hybridization with the out-of-plane In2 atoms is more important than the hybridization with the in-plane In1 atoms. This is in agreement with the results of the CeRh_{1- δ} Ir _{δ} In₅ substitution series¹⁵ where the orbitals that are more extended along the c -axis tend to hybridize more strongly. Nevertheless, the present results also show that hybridization with the In1 atoms is important and this supports the results of the CeCo(In_{1- y} Sn _{y})₅ substitution series;¹⁸ the Sn atoms go preferably to the In1 sites leading to a stronger hybridization in the plane.¹⁷

A modest increase in the contribution of $J_z = |\pm 5/2\rangle$ to the Γ_7^- -state of CeRhIn₅ will promote overlap of f -orbitals with p -states of In(1) at the expense f -In(2) hybridization. Mixing of Zeeman-split ground and Γ_7^+ first excited crystal field levels, in principle, could produce such a modest increase in the $J_z = |\pm 5/2\rangle$ contribution. Indeed, recent high-field magnetostriction³⁸ and nuclear magnetic resonance³⁹ measurements on CeRhIn₅ are consistent with this possibility that appears to be a significant contributing factor to field-induced Fermi-surface reconstruction in CeRhIn₅ subject to a magnetic field near 30 T.

In the limit of strong intra-atomic Coulomb interactions, which is typical of strongly correlated metals like CeCoIn₅ and CeRhIn₅, the magnetic exchange \mathcal{J} is proportional to the square of the matrix element $\langle V_{kf} \rangle$ that mixes conduction and f -wavefunctions.⁴⁰ Both Kondo and long-range Ruderman-Kittel-Kasuya-Yosida (RKKY) interactions depend on the magnitude of \mathcal{J} that is set by $\langle V_{kf} \rangle^2$ and, consequently, by the f -orbital configuration. These interactions are fundamental for a description of Kondo-lattice systems and their relative balance can be tuned by non-thermal control parameters, such as magnetic field and pressure. Modest pressure applied to CeRhIn₅ tunes its antiferromagnetic transition temperature toward zero temperature where a dome of unconventional superconductivity emerges with

a maximum transition temperature very close to that of CeCoIn₅⁴ and also changes the Fermi surface from small too large as in CeCoIn₅.⁸ We do not know if the f -orbital configuration of CeRhIn₅ at these pressures is the same as that of CeCoIn₅, but this is an interesting possibility that merits study.

VI. SUMMARY

In f -based materials, the shape of the crystal-field wavefunctions ultimately determines the origin of anisotropic hybridization in these materials and their ground state. Here, we show that the ground state of CeMIn₅ ($M = \text{Co, Rh}$) is a $\Gamma_7^- = |\alpha| |\pm 5/2\rangle - \sqrt{1 - \alpha^2} |\mp 3/2\rangle$ doublet with lobes Γ_7^- pointing toward the 110 direction, i.e., the lobes have xy character. Though careful DFT+DMFT calculations shed light on these materials, the crystal-field scheme obtained is different from our

experimental one. Our work settles the question on the orientation of f -orbitals in the doublet ground state of CeMIn₅ and will stimulate theoretical developments that take into account the actual wavefunctions.

VII. ACKNOWLEDGMENT

We thank Peter Thalmeier for fruitful discussions. Parts of this research were carried out at PETRA III/DESY, a member of the Helmholtz Association HGF, and we would like to thank Christoph Becker, Manuel Harder and Frank-Uwe Dill for skillful technical assistance. Work at Los Alamos was performed under the auspices of the U.S. Department of Energy, Office of Basic Energy Sciences, Division of Materials Science and Engineering. A.A., A.S., and M.S. gratefully acknowledge the financial support of the Deutsche Forschungsgemeinschaft under projects SE 1441-4-1.

* Present address: Bundesanstalt für Straßenwesen, Cologne, Germany

† Present address: Dipartimento di Fisica, Politecnico di Milano, Piazza Leonardo da Vinci 32, I-20133 Milano, Italy

‡ Present address: SLAC National Accelerator Lab., 2575 Sand Hill Rd, Menlo Park, CA 94025, USA

¹ H. v. Löhneysen, A. Rosch, M. Vojta, and P. Wölfle, “Fermi-liquid instabilities at magnetic quantum phase transitions,” *Rev. Mod. Phys.* **79**, 1015–1075 (2007).

² S. Wirth and F. Steglich, “Exploring heavy fermions from macroscopic to microscopic length scales,” *Nat. Rev. Mater.* **1**, 16066 (2016).

³ P. Coleman, *Handbook of Magn. and Adv. Magn. Mater.*, edited by M. Fähnle S. Maekawa H. Kronmüller, S. Parkin and I. Zutic, Vol. 1 (John Wiley and Sons, 2007) pp. 95–148, Heavy Fermions: Electrons at the Edge of Magnetism.

⁴ J. D. Thompson and Z. Fisk, “Progress in heavy-fermion superconductivity: Ce115 and related materials,” *J. Phys. Soc. Jpn.* **81**, 011002 (2012).

⁵ Y. Haga, Y. Inada, H. Harima, K. Oikawa, M. Murakawa, H. Nakawaki, Y. Tokiwa, D. Aoki, H. Shishido, S. Ikeda, N. Watanabe, and Y. Onuki, “Quasi-two-dimensional Fermi surfaces of the heavy fermion superconductor CeIrIn₅,” *Phys. Rev. B* **63**, 060503 (2001).

⁶ S.-I. Fujimori, T. Okane, J. Okamoto, K. Mamiya, Y. Muramatsu, A. Fujimori, H. Harima, D. Aoki, S. Ikeda, H. Shishido, Y. Tokiwa, Y. Haga, and Y. Onuki, “Nearly localized nature of f electrons in CeTIn₅ ($T = \text{Rh, Ir}$),” *Phys. Rev. B* **67**, 144507 (2003).

⁷ N. Harrison, U. Alver, R. G. Goodrich, I. Vekhter, J. L. Sarrao, P. G. Pagliuso, N. O. Moreno, L. Balicas, Z. Fisk, D. Hall, Robin T. Macaluso, and Julia Y. Chan, “ $4f$ -electron localization in Ce_xLa_{1-x}MIn₅ with $M = \text{Co, Rh, or Ir}$,” *Phys. Rev. Lett.* **93**, 186405 (2004).

⁸ H. Shishido, R. Settai, H. Harima, and Y. Onuki, “A drastic change of the Fermi surface at a critical pressure in CeRhIn₅: dHvA study under pressure,” *J. Phys. Soc. Jpn.* **74**, 1103 (2005).

⁹ R. Settai, T. Takeuchi, and Y. Onuki, “Recent advances in Ce-based heavy fermion superconductivity and Fermi surface properties,” *J. Phys. Soc. Jpn.* **76**, 051003 (2007).

¹⁰ H. Shishido, R. Settai, T. Kawai, H. Harima, and Y. Onuki, “de Haas-van Alphen effect of CeIr_{1-x}Rh_xIn₅,” *J. Mag. Mag. Mat.* **310**, 303 (2007).

¹¹ Swee K. Goh, J. P. Paglione, M. Sutherland, E. C. T. O’Farrell, C. Bergemann, T. A. Sayles, and M. B. Maple, “Fermi-surface reconstruction in CeRh_{1-x}Co_xIn₅,” *Phys. Rev. Lett.* **101**, 056402 (2008).

¹² M. P. Allen, F. Masee, D. K. Morr, J. Van Dyke, A. W. Rost, A. P. Mackenzie, C. Petrovic, and J. C. Davis, “Imaging Cooper pairing of heavy fermions in CeCoIn₅,” *Nat. Phys.* **9**, 468 (2013).

¹³ M. Sundermann, F. Strigari, T. Willers, J. Weinen, Y.F. Liao, K.-D. Tsuei, N. Hiraoka, H. Ishii, H. Yamaoka, J. Mizuki, Y. Zekko, E.D. Bauer, J.L. Sarrao, J.D. Thompson, P. Lejay, Y. Muro, K. Yutani, T. Takabatake, A. Tanaka, N. Hollmann, L.H. Tjeng, and A. Severing, “Quantitative study of the f occupation in CeMIn₅ and other cerium compounds with hard x-rays,” *J. Elec. Spec. and Rel. Phen.* **209**, 1 – 8 (2016).

¹⁴ P. G. Pagliuso, R. Movshovich, A. D. Bianchi, M. Nicklas, N. O. Moreno, J. D. Thompson, M. F. Hundley, J. L. Sarrao, and Z. Fisk, “Multiple phase transitions in Ce(Rh, Ir, Co)In₅,” *Physica B* **312-313**, 129 (2002).

¹⁵ T. Willers, F. Strigari, Z. Hu, V. Sessi, N.B. Brookes, E.D. Bauer, J.L. Sarrao, J.D. Thompson, A. Tanaka, S. Wirth, L.H. Tjeng, and A. Severing, “Correlation between ground state and orbital anisotropy in heavy fermion materials,” *Proc. Nat. Acad. Sci.* **112**, 2384–2388 (2015).

¹⁶ J. H. Shim, K. Haule, and G. Kotliar, “Modeling the localized-to-itinerant electronic transition in the heavy fermion system CeIrIn₅,” *Science* **318**, 1615 (2007).

¹⁷ H. Sakai, F. Ronning, J.-X. Zhu, N. Wakeham, H. Yasuoka, Y. Tokunaga, S. Kambe, E. D. Bauer, and J. D. Thompson, “Microscopic investigation of electronic inhomogeneity induced by substitutions in a quantum critical metal CeCoIn₅,” *Phys. Rev. B* **92**, 121105 (2015).

- ¹⁸ K. Chen, F. Strigari, M. Sundermann, Z. Hu, Z. Fisk, E. D. Bauer, P. F. S. Rosa, J. L. Sarrao, J. D. Thompson, J. Herrero-Martin, E. Pellegrin, D. Betto, K. Kummer, A. Tanaka, S. Wirth, and A. Severing, “Evolution of ground-state wave function in CeCoIn₅ upon Cd or Sn doping,” *Phys. Rev. B* **97**, 045134 (2018).
- ¹⁹ K. Haule, C.-H. Yee, and K. Kim, “Dynamical mean-field theory within the full-potential methods: Electronic structure of CeIrIn₅, CeCoIn₅, and CeRhIn₅,” *Phys. Rev. B* **81**, 195107 (2010).
- ²⁰ A. D. Christianson, J. M. Lawrence, P. G. Pagliuso, N. O. Moreno, J. L. Sarrao, J. D. Thompson, P. S. Riseborough, S. Kern, E. A. Goremychkin, and A. H. Lacerda, “Neutron scattering study of crystal fields in CeRhIn₅,” *Phys. Rev. B* **66**, 193102 (2002).
- ²¹ A. D. Christianson, E. D. Bauer, J. M. Lawrence, P. S. Riseborough, N. O. Moreno, P. G. Pagliuso, J. L. Sarrao, J. D. Thompson, E. A. Goremychkin, F. R. Trouw, M. P. Hehlen, and R. J. McQueeney, “Crystalline electric field effects in CeMIn₅ ($M=Co,Rh,Ir$): Superconductivity and the influence of Kondo spin fluctuations,” *Phys. Rev. B* **70**, 134505 (2004).
- ²² T. Willers, Z. Hu, N. Hollmann, P. O. Körner, J. Gegner, T. Burnus, H. Fujiwara, A. Tanaka, D. Schmitz, H. H. Hsieh, H.-J. Lin, C. T. Chen, E. D. Bauer, J. L. Sarrao, E. Goremychkin, M. Koza, L. H. Tjeng, and A. Severing, “Crystal-field and Kondo-scale investigations of CeMIn₅ ($M=Co, Ir, \text{ and } Rh$): A combined x-ray absorption and inelastic neutron scattering study,” *Phys. Rev. B* **81**, 195114 (2010).
- ²³ R.A. Gordon, M.W. Haverkort, S. Sen Gupta, and Sawatzky G.A., “Orientation-dependent x-ray Raman scattering from cubic crystals: Natural linear dichroism in MnO and CeO₂,” *J. Phys. Conf. Ser.* **190**, 012047 (2009).
- ²⁴ T. Willers, F. Strigari, N. Hiraoka, Y. Q. Cai, M. W. Haverkort, K.-D. Tsuei, Y. F. Liao, S. Seiro, C. Geibel, F. Steglich, L. H. Tjeng, and A. Severing, “Determining the in-plane orientation of the ground-state orbital of CeCu₂Si₂,” *Phys. Rev. Lett.* **109**, 046401 (2012).
- ²⁵ J.-P. Rueff, J. M. Ablett, F. Strigari, M. Deppe, M. W. Haverkort, L. H. Tjeng, and A. Severing, “Absence of orbital rotation in superconducting CeCu₂Ge₂,” *Phys. Rev. B* **91**, 201108 (2015).
- ²⁶ M. Sundermann, K. Chen, H. Yavas, Hanoh Lee, Z. Fisk, M. W. Haverkort, L. H. Tjeng, and A. Severing, “The quartet ground state in CeB₆: An inelastic x-ray scattering study,” *EPL* **117**, 17003 (2017).
- ²⁷ M. Sundermann, H. Yavas, K. Chen, D. J. Kim, Z. Fisk, D. Kasinathan, M. W. Haverkort, P. Thalmeier, A. Severing, and L. H. Tjeng, “4*f* crystal field ground state of the strongly correlated topological insulator SmB₆,” *Phys. Rev. Lett.* **120**, 016402 (2018).
- ²⁸ M. Sundermann, G. van der Laan, A. Severing, L. Simonelli, G. H. Lander, M. W. Haverkort, and R. Caciuffo, “Crystal-field states of UO₂ probed by directional dependence of nonresonant inelastic x-ray scattering,” *Phys. Rev. B* **98**, 205108 (2018).
- ²⁹ M. W. Haverkort, A. Tanaka, L. H. Tjeng, and G. A. Sawatzky, “Nonresonant inelastic x-ray scattering involving excitonic excitations: The examples of NiO and CoO,” *Phys. Rev. Lett.* **99**, 257401 (2007).
- ³⁰ R. A. Gordon, G. T. Seidler, T. T. Fister, M. W. Haverkort, G. A. Sawatzky, A. Tanaka, and T. K. Sham, “High multipole transitions in NIXS: Valence and hybridization in 4*f* systems,” *EPL (Europhysics Letters)* **81**, 26004 (2008).
- ³¹ J. A. Bradley, S. Sen Gupta, G. T. Seidler, K. T. Moore, M. W. Haverkort, G. A. Sawatzky, S. D. Conradson, D. L. Clark, S. A. Kozimor, and K. S. Boland, “Probing electronic correlations in actinide materials using multipolar transitions,” *Phys. Rev. B* **81**, 193104 (2010).
- ³² J. A. Bradley, K. T. Moore, G. van der Laan, J. P. Bradley, and R. A. Gordon, “Core and shallow-core *d*- to *f*-shell excitations in rare-earth metals,” *Phys. Rev. B* **84**, 205105 (2011).
- ³³ R. Caciuffo, G. van der Laan, L. Simonelli, T. Vitova, C. Mazzoli, M. A. Denecke, and G. H. Lander, “Uranium 5*d* – 5*f* electric-multipole transitions probed by nonresonant inelastic x-ray scattering,” *Phys. Rev. B* **81**, 195104 (2010).
- ³⁴ S. Huotari, Ch. J. Sahle, Ch. Henriquet, A. Al-Zein, K. Martel, L. Simonelli, R. Verbeni, H. Gonzalez, M.-C. Lagier, C. Ponchut, M. Moretti Sala, M. Krisch, and G. Monaco, “A large-solid-angle X-ray Raman scattering spectrometer at ID20 of the European Synchrotron Radiation Facility,” *J. Synchrotron Rad.* **24**, 521 (2017).
- ³⁵ M. W. Haverkort, “*Quantity* for core level spectroscopy - excitons, resonances and band excitations in time and frequency domain,” *J. Phys.: Conf. Ser.* **712**, 012001 (2016).
- ³⁶ R.D. Cowan, The theory of atomic structure and spectra. (University of California Press, 1981).
- ³⁷ A. Tanaka and T. Jo, “Resonant 3*d*, 3*p* and 3*s* photoemission in transition metal oxides predicted at 2*p* threshold,” *J. Phys. Soc. Jpn.* **63**, 2788 (1994).
- ³⁸ P. F. S. Rosa, S. M. Thomas, F. F. Balakirev, E. D. Bauer, R. M. Fernandes, J. D. Thompson, F. Ronning, and M. Jaime, “Enhanced hybridization sets the stage for electronic nematicity in CeRhIn₅,” *Phys. Rev. Lett.* **122**, 016402 (2019).
- ³⁹ G. G. Lesseux *et al.*, “Poster presentation, SCES meeting, Prague,” (2017).
- ⁴⁰ J. R. Schrieffer and P. A. Wolff, “Relation between the Anderson and Kondo Hamiltonians,” *Phys. Rev.* **149**, 491 (1966).